European Society of Computational Methods in Sciences, Engineering and Technology (ESCMSET)

Journal of Numerical Analysis, Industrial and Applied Mathematics (JNAIAM)
vol. 7, no. 1-2, 2012, pp. 39-57
ISSN 1790–8140

New Developments on Online Generation of Trajectories in Quadruped Robots [1]

Carla M.A. Pinto[2]*,Cristina P. Santos, Diana Rocha*, Vítor Matos****

* Instituto Superior de Engenharia do Porto
and Centro de Matemática da Universidade do Porto
Rua Dr António Bernardino de Almeida, 431,
4200-072 Porto, Portugal
cpinto@fc.up.pt

** Dept. Electrónica Industrial
and Centro Algoritmi Universidade do Minho
Campus de Azurém
4800-058 Guimarães, Portugal
cristina@dei.uminho.pt
vmatos@dei.uminho.pt

Received 30 January, 2011; accepted in revised form 19 June, 2012

Abstract: There has been considerable development in the design of efficient controllers for trajectory following in articulated robots with many degrees-of-freedom. Nevertheless generating trajectories online is still a complex and unsatisfactorily solved problem.
In this paper we present a new architecture for a Central Pattern Generator (CPG), for online generation of trajectories in quadruped robots. Our model is based on a CPG model for locomotor rhythms of quadruped animals, proposed by Golubitsky, Stewart, Buono, and Collins. Their model consists of eight coupled cells (CPG units) and each CPG unit is modeled as an oscillator by a system of ordinary differential equations (ODEs).
We generalize their CPG model, considering that each cell or CPG unit is divided in rhythmic and discrete motor primitives, modeled by simple nonlinear systems of ODEs. Superposition of discrete and rhythmic primitives may allow for more complex motor behaviours, namely locomotion in irregular terrain and obstacle avoidance. In this paper, the discrete primitive is inserted into the rhythmic one (i) as an offset of the solution, (ii) summed to the solution of the rhythmic primitive. We also consider three types of couplings between CPG units: synaptic, diffusive and mixed.
In this article we try to tackle the impact that these discrete corrections may have in the achieved system solutions. Numerical results show that amplitude and frequency of the periodic solutions are almost constant for all couplings in cases (i) and (ii). The larger variation occurs in the values of amplitude and frequency for case (i) in the synaptic coupling.
Results are also obtained in a robotic experiment using a simulated AIBO robot that walks over a ramp. Amplitude and frequency may be identified, respectively, with the range of motion and the velocity of the robots' movement.

© 2012 European Society of Computational Methods in Sciences, Engineering and Technology

[1] Published electronically June 30, 2012
[2] Corresponding author.

Keywords: Quadrupedal walking, Central Pattern Generator, Motor primitives, Changes in periodic solutions

Mathematics Subject Classification: Here must be added the AMS-MOS Subject Classification Index

PACS: Here must be added the PACS Numbers (if applicable)

1 Introduction

Animal locomotion, and more specifically, goal-directed locomotion, is a complex process, that is generally divided onto three distinct main subsystems, each playing a different role([9, 29, 15, 42, 48]). The generation of the rhythmic patterns is done by neural networks, the so-called central pattern generators (CPGs), located in the spinal cord. These networks send signals to the musculo-skeletal system, in order to produce torques in the different joints of the animals.The second subsystem, consisting of the brainstem command systems, integrates visual, sensory and vestibular inputs to control both steering and posture. The last subsystem, the basal ganglia, selects which motor primitive is activated at a given time. It has a very important role in determining which CPGs should be active at a given instant. The basal ganglia receives input from the cortex and the thalamus [26, 28].

In this paper we focus on the CPG locomotor models. CPGs are commomly modeled by coupled dynamical systems [8, 10, 6, 7, 43].

CPG-like coupled cell systems are able to produce sustained rhythmic activation patterns even when isolated from external stimuli [34]. This feature makes them suitable to model the control of legged robot locomotion for bipedal, quadrupedal and other designs. Other nice properties of dynamical systems are the low computational cost, the robustness against perturbations, smooth online modulation of trajectories, through changes in parameter values of the ODEs, and phase-locking between the different oscillators [51, 52, 16, 44, 4, 11]. It is also demonstrated that CPG-like controllers can be successfully implemented as analog electronic circuits [32].

Schöner *et al* [47] propose a set of organizational principles that allow an autonomous vehicle to perform stable planning, make planning decisions, and integrate redundant as well as complementary information. Yang *et al* [54] propose a biologically inspired neural network model to real-time collision-free motion planning of mobile robots or manipulators in a nonstationary environment. Righetti *et al* [45] use symmetric coupled systems theory ([19]) to design a generic coupling architecture for a CPG and show how it can be applied to the control of a crawling humanoid robot. Dégallier *et al* [11] use a dynamical systems' approach to do online generation of trajectories in a robot performing a drumming task. Nakamura *et al* [40] present a reinforcement learning method, labelled "CPG-actor-critic" method, based on the training of the CPG, allowing the biped robot not only to walk stably, but also to adapt to environmental changes. Lee *et al* [31] study a CPG-based analog controller, to generate adaptive walking motor programs of autonomous robots. Righetti *et al* [44] design a CPG architecture based on coupled dynamical systems where gait transition is achieved by parameter change and where sensory feedback is included. Zhang *et al* [55] present a bionic neural network model for fish-robot motion. This model consists of one high level controller and one chain of central pattern generators. Matos *et al* [36] propose a bio-inspired robotic controller able to generate locomotion and to easily switch between different types of gaits. The duty factor and the interlimb phase values are adjusted according to the velocities. This improves the robot stability and response during locomotion. Wu *et al* [53] use a biomimetic approach to control a snake-like robot with a large number of degrees of freedom. This method is based on networks of central pattern generators. These networks have a feedback term which can generate uniform outputs without any adjustment. Or [41] presents a new hybrid CPG-ZMP control system for the walking of a simulated flexible spine humanoid robot. His results show that the robot is able to adapt its spine motions in real-time to allow stable walking.

In this work, we focus on the design of a new CPG model, (quad-robot), for movement generation in a quadruped robot. It consists of eight symmetrically coupled CPG units.

The proposed CPG model quad-robot is based on a CPG for quadruped animals that was proposed by Golubitsky *et al* [21, 22]. Golubitsky *et al* [21, 22] prove that this is the minimal CPG capable of producing

© 2012 European Society of Computational Methods in Sciences, Engineering and Technology (ESCMSET)

the quadruped gaits of *walk*, *trot* and *pace* . Moreover, they also show that a CPG with a fewer number of cells, can not produce the rhythms associated to these gaits, in a biologically reasonable way. A CPG with four cells does not suffice, since *trot* and *pace* would be conjugated solutions symmetrically related and having the same stability properties. But *trot* and *pace* are distinct solutions, since, (1) camels and giraffes pace but do not trot, and horses trot and do not pace, unless taught [25, 30], and (2) stability of *trot* and *pace* is not the same [2]. Thus, it makes sense that minimal locomotor CPG networks for quadruped animals should have eight cells, that is, should have two cells for each leg.

Righetti *et al* [44, 45] propose CPG network models for quadruped robots with only four cells. Unwanted conjugacies between *trot* and *pace* presented in these CPG models force them to use different networks for generating all of the primary gaits of *bound*, *trot* , *walk*, and *pace*.

We assume a modular approach to movement generation, in which different combinations of a finite set of stable motor primitives organized at the spinal level result in movement generation [see [3] for a review]. In this article, motor primitives are defined relative to the movement they produce. They are simple commands from the brain that activate sets of muscles such that the resultant movement is as desired.

We assume two motor primitives, discrete and rhythmic. Further, we consider that each CPG unit is divided onto these two motor primitives, which are mathematically modelled by nonlinear dynamical systems. This movement decomposition and the chosen primitives are supported by current neurological and human motor control findings, specially considering the concepts of central pattern generators (CPGs) and force fields [see reviews by [3, 28]], and it has been often used in robotics both for generating movement and for selecting responses.

In [13] it was proposed a bio-inspired architecture functionally organized onto hierarchical layers according to their level of abstraction. This work applied the dynamical systems proposed in [11]. Such a simplified view of movement generation was further explored in [14] to reflect upon the potential differences between generation of discrete and rhythmic movements. They have proposed several mathematical models, based on the concept of motor primitives, according to four simple categories, that are able to produce both discrete and rhythmic trajectories.

In this article, we tackle a similar problematic, but the main focus relies on the different ways of embedding the generated motor primitives. We superpose both primitives using two different approaches. The discrete primitive is: i) added as an offset to the rhythmic primitive (similarly to the solution proposed in [11, 13, 36]); and ii) summed to the rhythmic primitive according to (similarly to the solution proposed in [12, 49]).

Furthermore, we also consider three types of couplings between the CPG units: synaptic, diffusive and mixed.

Several works in the robotics community have applied different models for movement generation based on the concept of motor primitives, but never addressed or explored which were effectively the changes introduced onto the systems solution when the discrete primitive target was changed. Herein, we vary the target of the discrete primitives and verify the obtained changes in the values of the amplitude and frequency of the achieved periodic solutions, for each primitive combination and type of coupling.

Amplitude and frequency may be identified, respectively, with the range of motion and the velocity of the robot's movements, when considering implementations of the proposed controllers for generating trajectories for the joints of real robots. Further, the adjustment of the target of the discrete primitive may be identified with postural control, locomotion over irregular terrains or obstacle avoidance, modelled as discrete, sensory driven corrections of the steady-state locomotion rhythmic patterns.

This article tries to show that these discrete corrections may be performed since that they do not affect the required amplitude and frequency of the resultant trajectories, nor the gait.

Numerical simulations results show that amplitude and frequency of the periodic solutions are almost constant for all couplings and combination of the two motor primitives.

A robotic experiment applies the proposed controller and shows the effectiveness of a controller that integrates both postural and rhythmic movement control. Trajectories generated by this controller are modulated by sensory feedback, according to the lateral tilt of the body similarly to work proposed by the authors in [49]. While walking the robot is faced with a ramp on its right side, which displaces its roll

© 2012 European Society of Computational Methods in Sciences, Engineering and Technology (ESCMSET)

angle. The robot moves forward but keeps its body almost parallel to the ground.

Outline of the paper

In section 2, we show the CPG architecture, the general class of ODEs that model the CPG quad-robot, and resume the symmetry techniques and bifurcation theory used in the classification of the periodic solutions produced by quad-robot, and their identification with quadruped locomotor patterns. In section 3, we simulate the CPG model using three distinct couplings and two ways of superposing the discrete and rhythmic primitives. We use the Hopf oscillator to model the rhythms and an inspired VITE model for the discrete primitive. In section 4, we perform a robotic experiment in which the proposed controller generates movements for locomotion and posture correction which are modulated according to sensory information. In section 5, we state the main conclusions and unravel some future research directions.

2 CPG Locomotion Model Architecture

In this section we introduce the CPG model for online generation of trajectories of quadruped robots. The CPG model is based in the CPG model for quadrupeds locomotor rhythms, proposed by Golubitsky *et al* [21, 22]. The eight coupled CPG units consist in two primitives: rhythmic and discrete. The superposition of rhythmic and discrete primitives allows for complex locomotor behaviour. We resume the symmetry techniques that allow classification of periodic solutions produced by the CPG model and identification with quadruped locomotor patterns.

2.1 CPG quadruped model design

In Figure 1 is it presented the CPG model quad-robot for generating locomotion for quadrupeds robots. It is based on a CPG for quadruped animals that was proposed by Golubitsky *et al* [21, 22]. The derivation of the CPG model by Golubitsky *et al* has a physiological interpretation. Each leg receives signals from two cells, in analogy to what happens in most animals' joints, where control is done mainly by two muscle groups.

Coupled cells networks can be represented by directed graphs whose nodes (cells) are identified with dynamical systems and whose edges (arrows) represent the couplings between them [50, 18, 17, 23, 19]. Different node/cell symbols represent distinct internal dynamics. Different couplings are drawn as different styles of edges/arrows. The CPG network model quad-robot in Figure 1 depicts an example of a coupled cells network in which the nodes are indicated by circles and arrows represent couplings.

The proposed model is a network of 8 coupled cells, LF_i (left fore leg cells), RF_i (right fore leg cells), LH_i (left hind leg cells), and RH_i (right hind leg cells), $i = 1,2$. The cells with $i = 2$ are considered a hidden layer. Each cell is a CPG unit and is divided onto two motor primitives, discrete and rhythmic, modelled by simple nonlinear dynamical systems.

The model has the bilateral symmetry of animals ($\mathbf{Z}_2(\kappa)$) and a cyclic translational symmetry ($\mathbf{Z}_4(\omega)$), from back to front, i.e, cell RF_2 is coupled to cell RH_1, and the same applies for cells LF_2 and LH_1.

The full symmetry group is the eighth order group given by:

$$\Gamma_{\mathsf{quad-robot}} = \mathbf{Z}_4(\omega) \times \mathbf{Z}_2(\kappa)$$

Symmetry seems a reasonable modeling assumption, though real life animals are not perfectly symmetric. Symmetry helps to explain, in particular, features like the phase of the gait cycle at which a given limb touches the ground, or the proportion of the gait cycle that a limb is in contact with the ground ('duty factor'). The phases and the duty factors help to distinguish and identify the gaits.

Moreover, there are particular phase relations in animals gaits. In a biped *walk*, left and right legs are half-period out of phase, a quadruped when performing a trot has diagonal pairs of legs moving synchronously, with the two pairs being half-period out of phase. In a hexapod metachronal gait, left and right legs are half-period out of phase. The major phase shifts observed in locomotor rhythms are simple

© 2012 European Society of Computational Methods in Sciences, Engineering and Technology (ESCMSET)

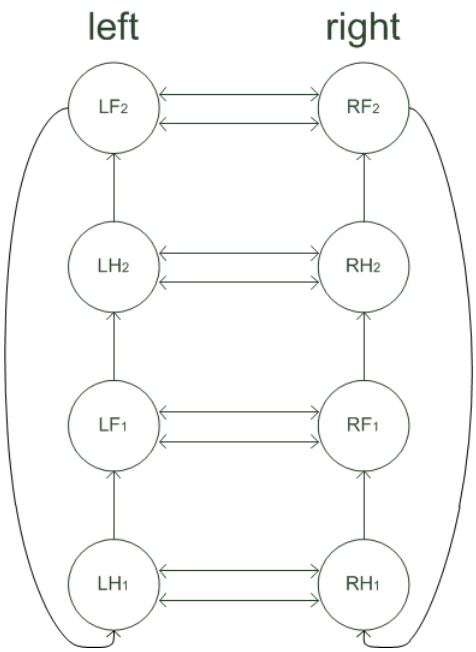

Figure 1: CPG locomotor model for quadrupeds, quad-robot. LF_i (left fore leg cells), RF_i (right fore leg cells), LH_i (left hind leg cells), RH_i (right hind leg cells), $i = 1,2$. Each leg receives signals from two cells (oscillators).

fractions of the period, suggesting that the model CPG might have some symmetry, since these particular phase shifts are unusual in asymmetric systems. CPG models for animals with a large number of identical segments, such as arthropods, should also have (maybe imperfect) translational symmetry, since 'identical segments' imply some degree of symmetry.

In Robotics, locomotor CPG networks for legged robots also show some degree of symmetry, namely bilateral [33, 52, 1] or dihedral symmetry [45, 44].

2.2 CPG model equations

The *network architecture* corresponds to a class of systems of differential equations [23]. Each of these systems can be considered to be a model CPG.

For example, the class of systems of differential equations of the CPG model for the quadruped model quad-robot is of the form:

$$\begin{aligned}
\dot{x}_{LH_1} &= F(x_{LH_1}, x_{RH_1}, x_{LF_2}) \\
\dot{x}_{RH_1} &= F(x_{RH_1}, x_{LH_1}, x_{RF_2}) \\
\dot{x}_{LF_1} &= F(x_{LF_1}, x_{RF_1}, x_{LH_1}) \\
\dot{x}_{RF_1} &= F(x_{RF_1}, x_{LF_1}, x_{RH_1}) \\
\dot{x}_{LH_2} &= F(x_{LH_2}, x_{RH_2}, x_{LF_1}) \\
\dot{x}_{RH_2} &= F(x_{RH_2}, x_{LH_2}, x_{RF_1}) \\
\dot{x}_{LF_2} &= F(x_{LF_2}, x_{RF_2}, x_{LH_2}) \\
\dot{x}_{RF_2} &= F(x_{RF_2}, x_{LF_2}, x_{RH_2})
\end{aligned} \tag{2.1}$$

where $x_i \in \mathbf{R}^k$ is the cell i variables, k is the dimension of the internal dynamics for each cell, and $F : (\mathbf{R}^k)^3 \to \mathbf{R}^k$ is an arbitrary mapping. The fact that the dynamics of each cell is modeled by the same function F indicates that the cells are assumed to be identical.

© 2012 European Society of Computational Methods in Sciences, Engineering and Technology (ESCMSET)

2.3 Spatio-temporal symmetries: brief review

In this section we review the concepts of spatial and spatiotemporal symmetries of periodic solutions of a system of differential equations. We then explain why these symmetries can be associated with gait patterns in animals locomotor CPG models.

Let Γ be a finite group of symmetries of the following systems of ODEs:

$$\frac{dx}{dt} = f(x) \tag{2.2}$$

Let $x(t)$ be a periodic solution of system 2.2, with period normalized to 1, and let $\gamma \in \Gamma$. By symmetry, we know that $\gamma x(t)$ is also a solution to (2.2). We consider two cases, either both solutions intersect (thus, are identical) or the two trajectories do not intersect.

Consider that both solutions are identical, then by uniqueness of solutions there is $\theta \in \mathbf{S}^1$ such that

$$\gamma x(t) = x(t-\theta) \quad \text{or} \quad \gamma x(t+\theta) = x(t)$$

and we say that $x(t)$ has spatio-temporal symmetry $\gamma \in \Gamma$, where θ is the temporal phase shift that corresponds to γ. If $\theta = 0$, then γ is a spatial symmetry.

Define K to be the subgroup of all spatial symmetries and H to be the subgroup of all spatiotemporal symmetries. Mathematically, we have:

$$\begin{array}{rcl} K & = & \{\gamma \in \Gamma : \gamma x(t) = x(t) \text{ for all } t\} \\ H & = & \{\gamma \in \Gamma : \gamma\{x(t)\} = \{x(t)\} \text{ for all } t\}. \end{array} \tag{2.3}$$

Next we discuss how symmetries of periodic solutions (H and K) in quad-robot (Figure 1) can correspond to the quadruped gaits of *bound* and *trot*. Let κ be the permutation that switches signals sent to left and right legs in quadrupeds. Applying κ to the *bound* does not change that gait since muscles groups in left and right legs receive the same set of signals. Applying κ to the *trot* does change the gait, in the sense that the muscle groups inside each leg receive signals that are now a half-period out of phase from the signals they received previously. The later implies that the legs are also half-period out of phase from where they were before applying κ. The permutation κ is called a *spatial* symmetry for the *bound* (the phase shift is zero) and is called a *spatiotemporal* symmetry for the *trot* (the phase shift is $1/2$). More precisely, applying κ to a *trot* and then performing a half-period phase shift does not change the *trot* gait.

Mathematically, suppose that $H = \Gamma_{\mathsf{quad-robot}}$ and $K = \mathbf{Z}_2(\kappa)$. Let $x(t) = (x_{LH_1}(t), \ldots, x_{RF_2}(t))$ be a 1-periodic solution with H and K symmetries. Since κ is a K symmetry the periodic solution must satisfy

$$\begin{array}{l} x_{LH_1}(t) = x_{LF_1}(t) = x_{LH_2}(t) = x_{LF_2}(t) \quad \text{and} \\ x_{RH_1}(t) = x_{RF_1}(t) = x_{RH_2}(t) = x_{RF_2}(t) \end{array}$$

Since ω is a spatiotemporal symmetry, $x_{RH_1}(t) = x_{LH_1}(t+\frac{1}{2})$. Thus

$$\begin{array}{c} x(t) = (x_{LH_1}(t), x_{LH_1}(t+\frac{1}{2}), x_{LH_1}(t), x_{LH_1}(t+\frac{1}{2}), \\ x_{LH_1}(t), x_{LH_1}(t+\frac{1}{2}), x_{LH_1}(t), x_{LH_1}(t+\frac{1}{2})) \end{array}$$

Note that the signals that go to muscle groups inside each leg are the same, whereas signals that go to the fore legs are half-period out of phase with the signals that go to the hind legs. Thus this rhythm is a *bound*.

The same reasoning applies to the *trot*, with $H = \Gamma_{\mathsf{quad-robot}}$ and $K = \mathbf{Z}_2(\omega\kappa)$.

Finally, we note that there is a mathematical theory that enables us to infer the CPG structure from the desired types of periodic solutions. The H/K Theorem [7] uses the symmetry group of a network to enumerate those pairs of spatiotemporal symmetry subgroups H and K that can correspond to periodic solutions of differential equations associated to the network.

© 2012 European Society of Computational Methods in Sciences, Engineering and Technology (ESCMSET)

2.4 Gaits produced by the CPG model

Gaits can be divided in two types: primary and secondary gait types. In primary gaits, muscle groups receive the same sinal up to a phase shift ($H = \Gamma_{\mathsf{quad-robot}}$) [7]. In secondary gaits muscle groups receive two different signals ($H \subset \Gamma_{\mathsf{quad-robot}}$) [6].

The proposed CPG model for quadrupeds, quad-robot, is the (unique) eight-cell network that can produce periodic solutions corresponding to the common quadrupedal gaits of *walk*, *trot*, and *pace* [21, 22]. Additionally, it predicts the *jump*, *bound*, *pronk*, and twelve more rhythmic locomotor patterns. In Tables 1-2, we write the symmetry pairs and the corresponding periodic solutions corresponding to common quadruped gaits.

H	K	**Name**
$\Gamma_{\mathsf{quad-robot}}$	$\Gamma_{\mathsf{quad-robot}}$	*pronk*
$\Gamma_{\mathsf{quad-robot}}$	$\mathbf{Z}_4(\omega)$	*pace*
$\Gamma_{\mathsf{quad-robot}}$	$\mathbf{Z}_4(\omega\kappa)$	*trot*
$\Gamma_{\mathsf{quad-robot}}$	$\mathbf{Z}_2(\omega^2\kappa)$	*walk*
$\mathbf{Z}_4(\omega)$	$\mathbf{Z}_2(\omega^2)$	*transverse gallop*
$\mathbf{Z}_4(\omega\kappa)$	$\mathbf{Z}_2(\omega^2)$	*rotary gallop*

Table 1: Symmetry pairs of periodic solutions identified with quadruped gaits.

LH	**RH**	**LF**	**RF**	**Name**
(x_{LH_1}, x_{LH_1})	(x_{LH_1}, x_{LH_1})	(x_{LH_1}, x_{LH_1})	(x_{LH_1}, x_{LH_1})	*pronk*
(x_{LH_1}, x_{LH_1})	$(x^S_{LH_1}, x^S_{LH_1})$	(x_{LH_1}, x_{LH_1})	$(x^S_{LH_1}, x_{LH_1})^S$	*pace*
(x_{LH_1}, x_{LH_1})	$(x^S_{LH_1}, x^S_{LH_1})$	$(x^S_{LH_1}, x^S_{LH_1})$	(x_{LH_1}, x_{LH_1})	*trot*
$(x_{LH_1}, x^S_{LH_1})$	$(x^S_{LH_1}, x_{LH_1})$	$(x^{SS}_{LH_1}, x^{SSS}_{LH_1})$	$(x^{SSS}_{LH_1}, x^{SS}_{LH_1})$	*walk*
(x_{LH_1}, x_{LH_1})	(x_{RH_1}, x_{RH_1})	$(x^S_{LH_1}, x^S_{LH_1})$	$(x^S_{RH_1}, x^S_{RH_1})$	*transv. gal.*
(x_{LH_1}, x_{LH_1})	(x_{RH_1}, x_{RH_1})	$(x^S_{RH_1}, x^S_{RH_1})$	$(x^S_{LH_1}, x^S_{LH_1})$	*rot. gal.*

Table 2: Periodic solutions identified with quadruped gaits, where period of solutions is normalized to 1. Each leg receives a pair of periodic solutions, from (non hidden, hidden)) layers. ^{S} is half period out of phase, ^SS is a quarter of period out of phase and ^SSS is three quarters of period out of phase.

A CPG model with a fewer number of cells cannot predict gaits like *walk*, *trot*, and *pace*. In this case, it is necessary to consider different architectures, with different symmetry groups, in order to obtain all of the quadruped usual gaits. In these models, each leg receives only one signal. Collins and Stewart [10] describe 5 different architectures for a CPG model for quadruped rhythms. Each of these network models has a distinct symmetry type. All together, these CPG models predict gaits like *walk*, *trot*, and *pace*. Nevertheless, it is not expected that animals switch between distinct CPG models in order to switch gaits. Moreover, in these networks *trot* and *pace* exist simultaneously and have the same stability properties, being conjugated solutions. As it is proved that (1) camels and giraffes pace but do not trot, and horses trot and do not pace, unless taught [25, 30], and (2) stability of *trot* and *pace* is not the same [2], then *trot* and *pace* must not be conjugated solutions.

3 Numerical Simulations

We simulate the CPG model quad-robot. We use a modified Hopf oscillator [24, 35] to model cell's rhtyhmic internal dynamics and another system of ordinary differential equations, based in the VITE model [5], for the discrete primitive.

© 2012 European Society of Computational Methods in Sciences, Engineering and Technology (ESCMSET)

The superposition of discrete and rhythmic primitives is done using two distinct approaches. The discrete primitive, $y(t)$, is: (i) added as an offset of the rhythmic solution $x(t)$; (ii) summed to the solution $x(t)$. We also consider three types of coupling between CPG units : synaptic, diffusive and mixed. We vary parameter g and compute, for each value of g, the amplitude and the frequency of two periodic solutions, identified with the quadruped rhythms of *trot* and *pace*.

Numerical results are illustrated.

3.1 CPG model quad-robot

In our CPG model quad-robot , each CPG unit (or cell) combines two motor primitives, discrete and rhythmic, modeled as simple nonlinear dynamical systems. The rhythmic motor primitive is modeled by a modified Hopf oscillator [24, 35], and another system of ordinary differential equations, based in the VITE model [5], models the discrete primitive.

Discrete primitives

The system of ordinary differential equations that models the discrete primitive is given by:

$$\begin{aligned} \dot{h} &= d(p-h) \\ \dot{y} &= h^4 v \\ \dot{v} &= p^{\frac{4-b^2}{4}}(y-g) - bv \end{aligned} \tag{3.4}$$

where y converges asymptotically and monotonically to a goal g. The speed of this convergence is controlled by b and v is the bell-shape velocity curve. h converges to p and is reset to zero at the end of each movement.

Rhythmic primitive

Modified Hopf oscillators have been used in the generation of the rhythmic primitive of robots trajectories [11, 45, 44, 36]. The equations for the single Hopf oscillator are given by:

$$\begin{aligned} \dot{x} &= \alpha(\mu - r^2)x - \omega z = f(x,z) \\ \dot{z} &= \alpha(\mu - r^2)z + \omega x = g(x,z) \end{aligned} \tag{3.5}$$

where $r^2 = x^2 + z^2$, $\sqrt{\mu}$ is the amplitude of the oscillation. For $\mu < 0$ the oscillator is at a stationary state, and for $\mu > 0$ the oscillator is at a limit cycle. At $\mu = 0$ it occurs a Hopf bifurcation.

Parameter ω is the intrinsic frequency of the oscillator, α controls the speed of convergence to the limit cycle. ω_{swing} and ω_{stance} are the frequencies of the swing and stance phases, $\omega(z) = \frac{\omega_{stance}}{\exp(-az)+1} + \frac{\omega_{swing}}{\exp(az)+1}$ is the intrinsic frequency of the oscillator (verify [45] for more details).With this ODE system, we can explicitly control the ascending and descending phases of the oscillations as well as their amplitudes, by just varying parameters ω_{stance}, ω_{swing} and μ.

Superposition of rhythmic and discrete primitives

The superposition of discrete and rhythmic primitives is herein done using two distinct approaches, summarized in Figure 2. The discrete primitive, $y(t)$ is: (i) added as an offset of the rhythmic solution $x(t)$; (ii) summed to the solution $x(t)$.

Case (i)

In this case, the discrete primitive is embedded onto the rhythmic one as an offset and their superposition is given by:

$$\begin{aligned} \dot{x}_i &= \alpha(\mu - r_i^2)(x_i - y_i) - \omega z_i = f_1(x_i, z_i) \\ \dot{z}_i &= \alpha(\mu - r_i^2)z_i + \omega(x_i - y_i) = g_1(x_i, z_i), \end{aligned} \tag{3.6}$$

© 2012 European Society of Computational Methods in Sciences, Engineering and Technology (ESCMSET)

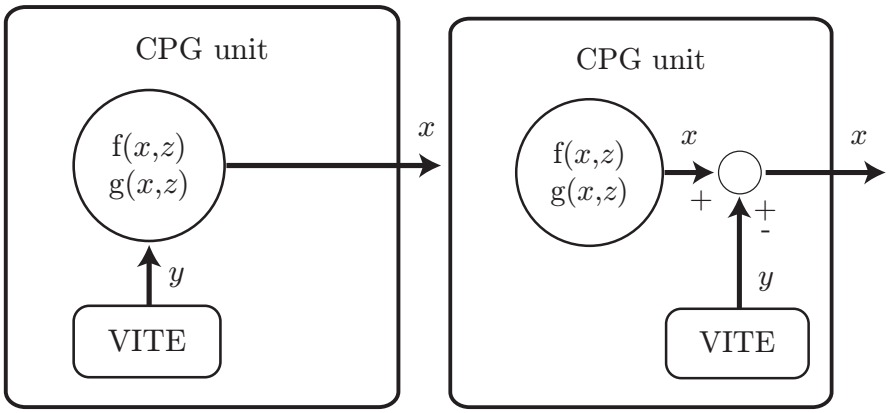

(a) case i) (b) case ii)

Figure 2: CPG unit of a CPG locomotor model for quadruped robots (quad-robot). (left) case (i). (right) case (ii).

where $r_i^2 = (x_i - y_i)^2 + z_i^2$.

In this system, similar to the one presented in drumming [11] and extended in [36] both discrete and rhythmic primitives are generated through a unique set of differential equations. The system bifurcates between a unique point attractor and a limit cycle according to one single parameter, μ. It is believed that this design enables to produce more complex movements modelled as periodic movements around time varying offsets.

Case (ii)

In this case, the discrete primitive $y_i(t)$ is summed to the solution of the single Hopf oscillator given by Eq. 3.5, as $x_i(t) - y_i(t)$ or as $x_i(t) + y_i(t)$.

CPG Network

We consider three types of coupling between CPG units: synaptic, diffusive and mixed. The coupled systems of ODEs that model CPG quad-robot for diffusive, synaptic and mixed couplings are given by:

$$\begin{aligned} \dot{x}_i &= f_2(x_i, z_i) + k_1 h_1(x_{i-2}, x_i) + k_2 h_2(x_{i+\varepsilon_i}, x_i) \\ \dot{z}_i &= g_2(x_i, z_i) + k_3 h_2(z_{i-2}, z_i) + k_4 h_2(z_{i+\varepsilon_i}, z_i) \end{aligned} \tag{3.7}$$

where $f(x_i, z_i)$, $g(x_i, z_i)$, and r_i^2 are as defined by Eq. 3.6 for case (i), and by the single Hopf oscillator (Eq. 3.5) for case (ii), $\varepsilon_i = (-1)^{i+1}$, and indices are taken modulo 8. Function $h_l(x_i, x_j)$, $l = 1,2$, represents synaptic coupling when written in the form $h_l(x_i, x_j) = x_j$, $l = 1,2$, and diffusive coupling when written as $h_l(x_i, x_j) = x_j - x_i$, $l = 1,2$. Functions $h_1(x_i, x_j) = x_i - y_i$ and $h_2(x_i, x_j) = x_j$ indicate mixed coupling. For case (i), we let $f_2(x_i, z_i) = f_1(x_i, z_i)$ and $g_2(x_i, z_i) = g_1(x_i, z_i)$. For case (ii), we consider $f_2(x_i, z_i) = f(x_i, z_i)$ and $g_2(x_i, z_i) = g(x_i, z_i)$.

3.2 Simulations

We simulate the CPG model quad-robot, for $t = 128$. Parameter values used in the simulations are $\mu = 10.0$, $\alpha = 5$, $\omega_{\text{stance}} = 6.2832\ \text{rads}^{-1}$, $\omega_{\text{swing}} = 6.2832\ \text{rads}^{-1}$, $a = 50.0$.

© 2012 European Society of Computational Methods in Sciences, Engineering and Technology (ESCMSET)

Amplitude and frequency of periodic solutions

Figures 3.2- 3.2 show amplitude (TOP) and frequency (BOTTOM) values produced by CPG quad-robot and identified with *pace* (left) and *trot* (right), for varying $g \in [-25, 25]$ in steps of 0.1, in cases (i) (dashed line) and (ii) (filled line) for synaptic and mixed coupling, respectively. The values of g not plotted in the graphs are those for which the solution goes to equilibrium. The diffusive coupling graphs have shown horizontal lines for all the graphs. Thus frequency and amplitude are independent of the variation of the goal value.

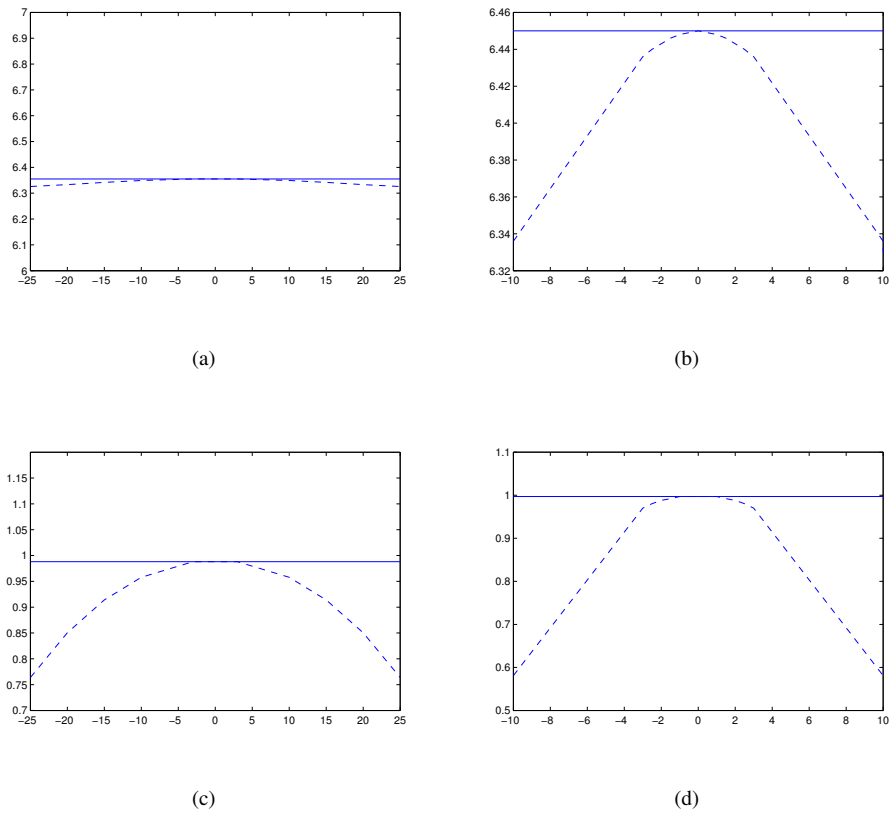

Figure 3: Amplitude (TOP) and frequency (DOWN) of the periodic solutions produced by CPG quad-robot and identified with *pace* (LEFT) and *trot* (RIGHT), for varying $g \in [-25, 25]$ in steps of 0.1, in cases (i) (dashed line) and (ii) (filled line) for synaptic coupling. For more information see text.

We verify that *trot* and *pace* periodic solutions are not affected in terms of time of convergence for the different cases of discrete and rhythmic superposition. Main differences arise in the offset of the solutions.

In all three cases, the amplitude and frequency are almost constant. The cases where there is more variation of amplitude and frequency values is when the coupling is either synaptic or mixed and the discrete primitive is inserted into the rhythmic one as an offset (case (i)).

Absolute error

Figure 5 depicts the absolute values of the error in the amplitude values of the purely rhythmic periodic solutions, identified with the quadruped gaits of *pace* (LEFT) and *trot* (RIGHT), when the discrete primitive

© 2012 European Society of Computational Methods in Sciences, Engineering and Technology (ESCMSET)

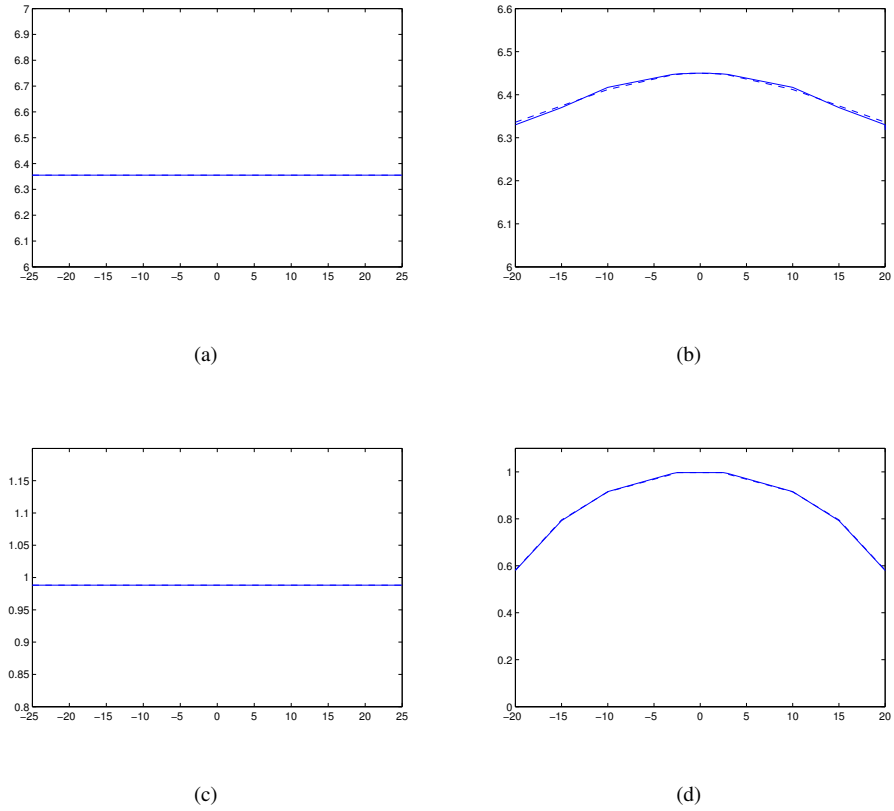

Figure 4: Similar to Figure 3.2 but for mixed coupling. For more information see text.

is inserted as in case (i) (TOP) and in case (ii) as $x_i(t) \pm y_i(t)$ (BOTTOM), for varying values of g (x-axis), for diffusive (solid line), synaptic (dashed line) and mixed (dashed-dotted line) coupling.

Absolute values of the error in the frequency values are depicted in Figure 6. Note that when the discrete primitive is inserted as in case (ii), absolute error values in the amplitude and frequency were identical for insertion as $x_i(t) \pm y_i(t)$.

We have computed the trendline that better describes the error function. We have found that it has quadratic form for all types of coupling and for the three forms of inserting the discrete primitive into the rhythmic one. These trendlines are surveyed in table 3. These figures enable us to draw the following conclusions. (1) The error is zero for diffusive coupling. (2) If there is error, for synaptic (*trot* and *pace*) and mixed (*trot*) types of coupling, the error is as high as the absolute value of g. Precisely, the error varies in a quadratic form with g, and is zero for $g = 0$. (3) When the discrete primitive is summed to the solution of the rhythmic part (case ii)), the obtained solutions seem to present a smaller error.

Discussion

In survey, from the observation of the graphs, we conclude that the coupling that provides the best result is the diffusive coupling. In this case, there is no difference between cases (i) and (ii). A possible explanation for this fact is that the transient of the periodic solution, obtained after insertion of the discrete part (for $t = 128$), is smaller for the case of diffusive coupling than for the cases of synaptic and mixed couplings. It means that, for the later, there is a bigger perturbation of the rhythmic part, caused by the discrete primitive.

© 2012 *European Society of Computational Methods in Sciences, Engineering and Technology (ESCMSET)*

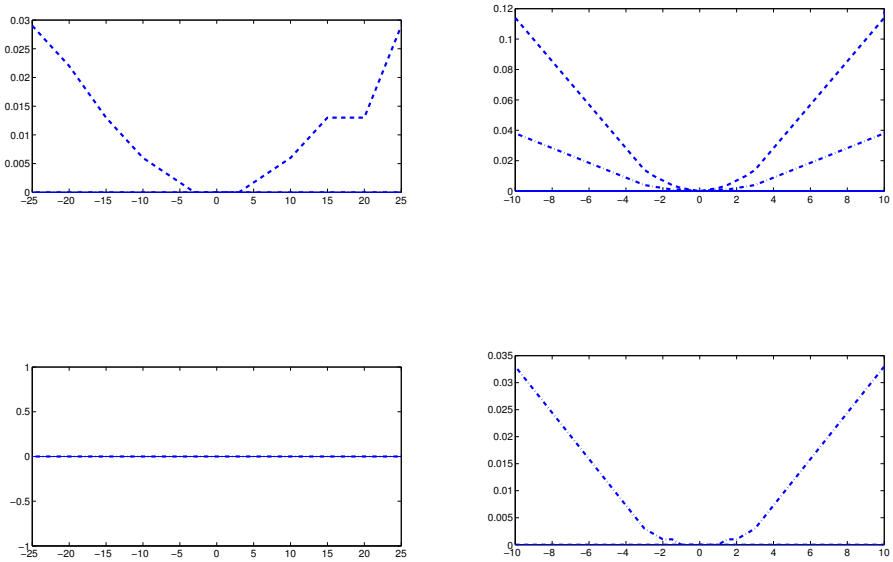

Figure 5: Absolute error in the amplitude values of the periodic solutions produced by CPG quad-robot and identified with *pace* (LEFT) and *trot* (RIGHT), for varying g, for diffusive (filled line), synaptic (dashed line) and mixed (dashed-dotted line) coupling, when the discrete primitive is inserted as in case i) (TOP) and as in case ii), as $f(x_i(t), z_i(t)) - y_i(t)$ (BOTTOM).

Nevertheless, from a mathematically point of view, if simulated these solutions for more time, then this transient would disappear and there wouldn't be any differences in amplitude and frequency values. The periodic solution tends asymptotically for a solution with the same amplitude and frequency than before, but with a different offset. This fact will be explained in a future work.

In general, the case that performs the best for all couplings is case (ii), where the discrete primitive is summed to the solution of the rhythmic one. By 'best', we mean that the amplitude and frequency values of the achieved periodic solutions, obtained after superimposing the discrete to the rhythmic primitive, are not or are only slightly affected. Therefore, it is possible to use them for generating trajectories for the joint values of real robots, since varying the joint offset will not affect the required amplitude and frequency of the resultant trajectory, nor the gait.

CARLA: Could authors give any mathematical reason for such kind of dynamical behaviour to occur?

Table 3: Values for the quadratic forms of error trendlines for all types of coupling and combination of discrete and rhythmic primitives. R^2 is the square of the correlation coefficient.

		Amplitude			Frequency		
		Synaptic	Diffusive	Mixed	Synaptic	Diffusive	Mixed
Trot	Case (i)	$y = 0.0011x^2$ $R^2 = 0.9969$	0	$y = 0.0003x^2$ $R^2 = 0.987$	$y = 0.0041x^2$ $R^2 = 0.9979$	0	$y = 0.001x^2$ $R^2 = 0.9928$
	Case (ii) $x \pm y$	0	0	$y = 0.0003x^2$ $R^2 = 0.992$	0	0	$y = 0.001x^2$ $R^2 = 0.9931$
Pace	Case (i)	$y = 0.00005x^2$ $R^2 = 0.9739$	0	0	$y = 0.0003x^2$ $R^2 = 0.964$	0	0
	Case (ii) $x \pm y$	0	0	0	0	0	0

© 2012 European Society of Computational Methods in Sciences, Engineering and Technology (ESCMSET)

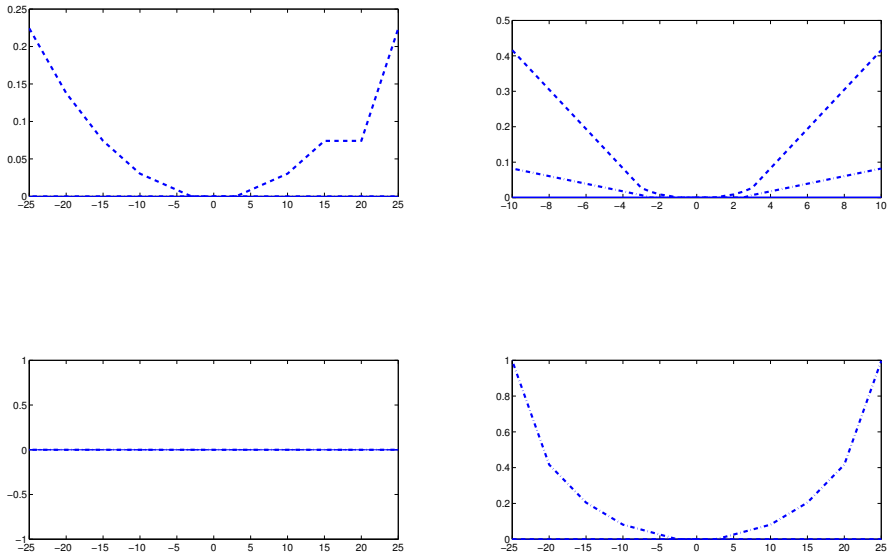

Figure 6: Similar to figure 5 but for the absolute value of the error in the frequency values.

4 Robotic Experiment

Several experiments were performed to verify the adequacy of the locomotor CPG network to movement generation. Experiments were performed on the webots [37] robotics simulator. Webots is a software for the physic simulation of robots based on ODE, an open source physics engine for simulating 3D rigid body dynamics.

4.1 Robotic setup

In this work we use a simulated AIBO ERS-7 quadruped robot manufactured by Sony to demonstrate the feasibility of the proposed system. The AIBO dog robot is a 18 DOFs quadruped robot that, unlike its natural counterpart, has three joints per limb, with different configurations of a real dog limbs. Besides, the robot body and limbs are rigid with non-compliant servo joints. The joints are stiff, without any elasticity, and their position is specified by an angle value. The durations of the achieved step phases have to be limited, because the joints present timing constraints on movement executions.

We control the four hip-swing degrees-of-freedom (DOFs) (fig. 7).

The AIBO has a 3-axis accelerometer built into its body that enables us to calculate the lateral tilt (roll) of the robot body.

4.2 Postural Control

The proposed postural control system generates movements both for locomotion generation and for posture correction and it is based on past work [49]. It enables integration of sensory feedback such that movements are robustly generated and adapted to the environment.

This controller is modeled by the previous described autonomous differential equations, whose intrinsic properties provide for the required features. For instance, sensory information is noisy and changes as a result of the generated robot movement.

© 2012 *European Society of Computational Methods in Sciences, Engineering and Technology (ESCMSET)*

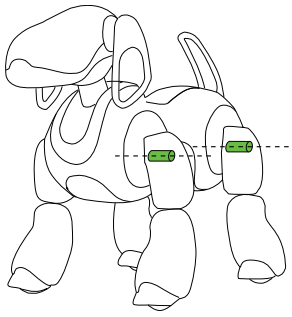

Figure 7: Schematic view of the ERS-7 AIBO model depicting the controlled swing DOFs for the left side.

The objective of this controller is to adjust the body inclination, opposing to changes in terrain slope, so that the roll is reduced to a minimum. Slope compensation is achieved through extension and flexion of the legs, changing the legs height , according to the offset y_i value given by the discrete primitive.

For offset y_i specification, we measure the lateral tilt of the body, ϕ. We want to stretch the legs towards which the robot is tilted, and fold the other legs, thus reducing the robot lateral tilt and keeping the body parallel to the ground. This is achieved by reducing the swing joint values of the former and increasing these joint values for the later. The effect of this offset joint change should be of opposite effect on the left and right legs of the robot, but should also influence similarly both legs. This postural correction is illustrated in fig. 8.

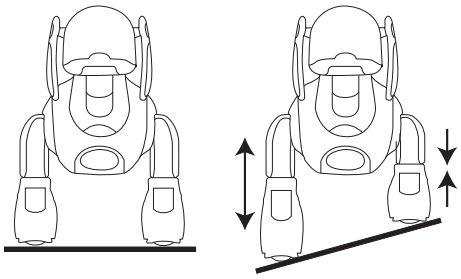

Figure 8: Robot's roll angle is adjusted by extending/flexing the front/rear legs in coordination.

The final trajectories x_i specify the planned swing joint values needed to reduce the lateral tilt to a minimum. These are sent online for each DOF and the lower level control is done by PID controllers. Because motion is sufficiently slow there is no need to apply inverse dynamics.

We set the frequency to $\omega_{\mathrm{sw}} = 6.28\ \mathrm{rad.s}^{-1}$ in regards with the motor limitations. Further, the dynamical parameters controlling the speed of convergence of unit-CPGs were set to $\frac{1}{2\,\alpha_{\mathrm{i}}\,\mu_{\mathrm{i}}} = 0.01$ s, in regard to stability during the integration process and to feasibility of the desired trajectories.

At each sensorial cycle, dynamic equations are calculated and numerically integrated using the Euler method with a fixed time step of 1 ms, thus specifying servo positions. The robot control loop is measured and has 8 ms.

4.3 Experiments

Many possible motions were experimented over several runs by specifying different offset values of the joints. Due to space constraints, we only depict a more complex experiment in which while walking the robot is faced with a ramp on its right side, displacing its roll angle. The ramp inclines the robot towards the side. It is expected that the robot keeps moving forward but tries to suppress the ramp inclination to

© 2012 European Society of Computational Methods in Sciences, Engineering and Technology (ESCMSET)

values near zero, by adjusting the offset value of the generated trajectories, keeping the body parallel to the ground.

The robot behaves as expected and moves forward over the ramp but keeping its body almost parallel to the ground. Fig. 9 provides for a visual comparison of the experiment when there is (TOP) and there is no (BOTTOM) roll compensation as snapshots at time $t = 5$ s, $t = 15$ s and $t = 25$ s. The overall experiment can be seen in the attached video.

Note that the ramp has an inclination adequate to the robot size. The role of the feedback is to keep the body parallel to the ground while locomoting. Larger values of the ramp would make it impossible for the robot to go ahead with its body parallel to the ground.

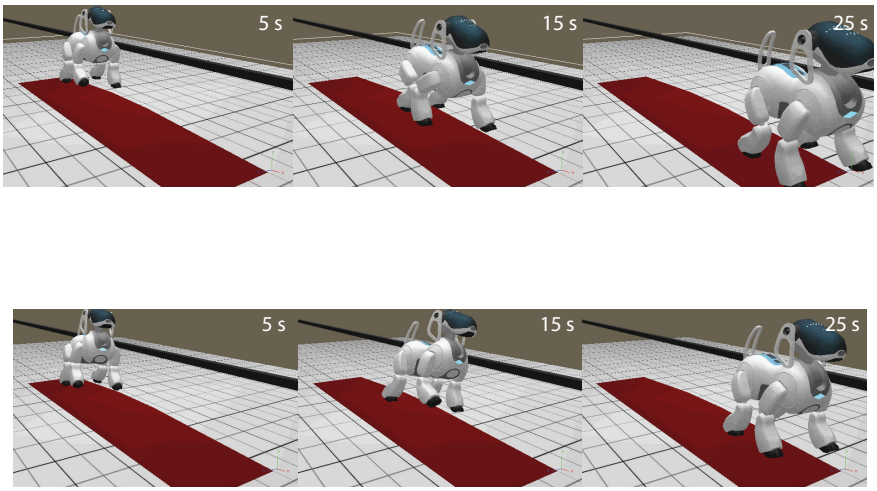

Figure 9: Snapshots showing that while walking the robot is faced with a ramp on its right side. TOP: The robot compensates the ramp inclination by adjsuting the offset value of the swing trajectories. BOTTOM: The robot inlcines with the ramp because there is no postural correction system for roll compensation.

Fig 10 depicts time courses of the roll (TOP) and of the generated left (MIDDLE) and right (BOTTOM) hip swing trajectories for both fore legs. Solid and dotted lines correspond to data acquired when there is and there is not roll compensation, respectively.

The robot roll angle shows a displacement of almost 10° while the robot walks over the ramp (dotted line, top panel), from 5 s to 10 s, and the ramp inclination is positive.

This roll angle displacement is suppressed when the roll compensation is activated (solid line, top panel), by means of changing leg height through offset modulation (solid lines, bottom panels).

Left and right fore offsets are changed symmetrically, the left legs are extended (cyan line, middle panel) and the right legs are flexed (yellow line, bottom panel), changing the posture of the robot's body while walking over the ramp suppressing the roll displacement to around 0° (solid line, top panel).

At $t \approx 20s$, the ramp inclination becomes negative and the robot starts to move downhill. The postural control tries to take the roll towards zero during the robot movement by flexing the left legs and extending the right ones to the original posture.

5 Conclusion

We propose a new CPG locomotor model for quadruped robots patterns. This model is based in a CPG model for quadrupeds, developed by Golubitsky *et al*. We consider that the CPG model consists of eight

© 2012 *European Society of Computational Methods in Sciences, Engineering and Technology (ESCMSET)*

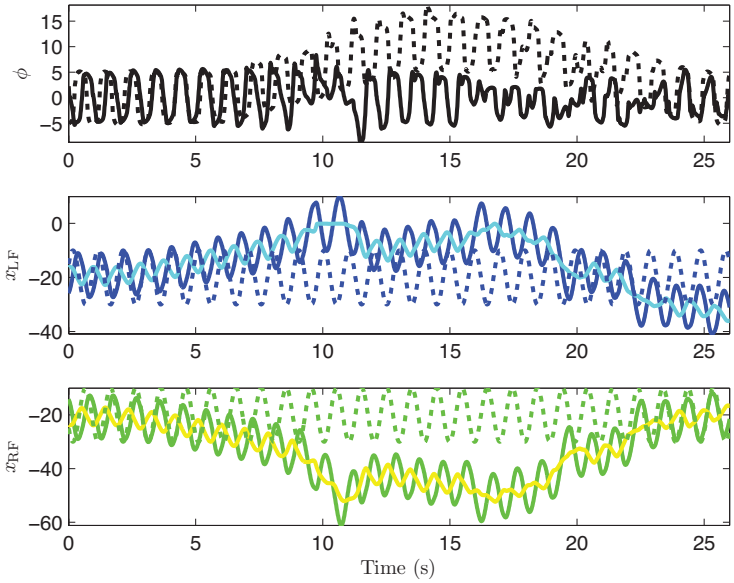

Figure 10: Time courses of variables corresponding to the experiment depicted in fig. 9. Solid and dotted lines correspond to data acquired when there is and there is not roll compensation, respectively. TOP: roll; MIDDLE: left fore hip swing trajectory; and BOTTOM: right fore hip swing trajectory.

coupled CPG units, where each CPG unit combines two motor primitives, discrete and rhythmic.

We simulate the CPG model considering two distinct ways of superimposing the discrete and rhythmic primitive and for three distinct coupling functions. For each case, we compute the amplitude and the frequency values of the periodic solutions identified with *trot* and *pace*, for values of the discrete primitive target parameter $g \in [-25, 25]$. Numerical results show that amplitude and frequency values are almost constant. The cases where there is more variation for these values is when the coupling is either synaptic or mixed and the discrete primitive is inserted into the rhythmic primitive as an offset (case (i)). The coupling that provides the best result is the diffusive coupling. In this case there is no difference between cases (i) and (ii). In general, the case that performs the best for all couplings is case (ii), where the discrete primitive is summed to the solution of the rhythmic one.

The controller is also validate in a robotic experiment where adjustment of the target of the discrete primitive is identified with postural control, that models as discrete, lateral tilt driven corrections the steady-state locomotion rhythmic patterns.

Acknowledgments

CS and VM were supported by FCT through the Centro de Investigação ALGORITMI da Universidade do Minho. All authors were supported by FEDER Funding, by the Operational Program Competitive Factors COMPETE, and National Funding supported by the FCT - Portuguese Science Foundation through project PTDC/EEACRO/100655/2008.

References

[1] A.G. Baydin. Evolution of central pattern generators for the control of a five-link planar bipedal walking mechanism. *arXiv:0801.0830v3* (2008).

© 2012 European Society of Computational Methods in Sciences, Engineering and Technology (ESCMSET)

[2] J. Blaszczyk, C. Dobrzecka. Alteration in the pattern of locomotion following a partial movement restraint in puppies. *Acta. Neuro. Exp.* **49** (1989) 39-46.

[3] E. Bizzi, A d'Avella, P Saltiel and M Trensch. Modular organization of spinal motor systems. *The Neuroscientist* **8** No 5 (2002) 437–442.

[4] M. Bühler and S. Koditscheck. Planning and control of juggling robot. *Int. J. of Robotics Research* **13** (2) (1994) 101–118.

[5] D. Bullock and S. Grossberg. *The VITE model: a neural command circuit for generating arm and articulator trajectories.* In J. Kelso, A. Mandell, and M. Shlesinger, editors, Dynamic patterns in complex systems, pages 206-305. Singapore: World Scientific, (1988).

[6] P.L. Buono. Models of central pattern generators for quadruped locomotion II. Secondary gaits, *J. Mathematical Biology* **42** No 4 (2001) 327–346.

[7] P.L. Buono and M. Golubitsky. Models of central pattern generators for quadruped locomotion I. Primary gaits, *J. Mathematical Biology* **42** (2001) 291–326.

[8] A.H. Cohen, P.J. Holmes, and R.H. Rand. The nature of the coupling between segmental oscillators of the lamprey spinal generator for locomotion: a mathematical model., *J. Math. Biol.* **13** No 3 (1982) 345–369.

[9] A.H. Cohen, G.B. Ermentrout, T. Kiemel, N. Kopell, K.A. Sigvardt, and T.L. Williams. Modelling of intersegmental coordination in the lamprey central pattern generator for locomotion, *Trends in Neuroscience* **15** No 11 (1992) 434–438.

[10] J.J. Collins and I. Stewart. Coupled nonlinear oscillators and the symmetries of animal gaits, *J. Nonlin. Sci.* **3** (1993) 349–392.

[11] S. Degallier, C.P. Santos, L. Righetti, and A. Ijspeert. Movement Generation using Dynamical Systems: A Drumming Hummanoid Robot. Humanoid's06 IEEE-RAS International Conference on Humanoid Robots. Genova, Italy (2006).

[12] S. Degallier, L. Righetti, and A. Ijspeert. Hand placement during quadruped locomotion in a humanoid robot: A dynamical system approach. In *Proceedings of the IEEE-RAS International Conference on Intelligent Robots and Systems (IROS07)*, San Diego, (2007).

[13] S. Degallier, L. Righetti, L. Natale, F. Nori, G. Metta and A. Ijspeert. A modular bio-inspired architecture for movement generation for the infant-like robot iCub. *BioRob* (2008).

[14] S. Degallier and A. Ijspeert. Modeling discrete and rhythmic movements through motor primitives: a review. *Biological Cybernetics* **103** (2010) 319–338.

[15] A.W. English. Interlimb coordination during stepping in the cat: an electromyographic analysis, *J. Neurophysiology* **42** Issue 1 (1979) 229–243.

[16] Y. Fukuoka, H Kimura, and A. Cohen. Adaptive walking of a quadruped robot o irregular terrain based on biological concepts. *Int. J. of Robotics Research* **3–4** (2003) 187–202.

[17] M. Golubitsky, M. Nicol and I. Stewart. Some curious phenomena in coupled cell systems. *J. Nonlinear Sci.* **14** 207–236. (2004)

[18] M. Golubitsky, M. Pivato, I. Stewart. Interior symmetry and local bifurcation in coupled cell networks, *Dyn Syst*, **19**, 389-407. (2004)

© *2012 European Society of Computational Methods in Sciences, Engineering and Technology (ESCMSET)*

[19] M. Golubitsky, I. Stewart. Nonlinear dynamics of networks: the groupoid formalism, *Bull. Amer. Math. Soc.*, **43** (2006) 305–364.

[20] M. Golubitsky and I. Stewart. *The Symmetry Perspective*, Progress in Mathematics **200**, Birkhauser, Basel, 2002.

[21] M. Golubitsky, I. Stewart, P.L. Buono, and J.J. Collins. A modular network for legged locomotion. *Physica D* **115** (1998) 56–72.

[22] M. Golubitsky, I. Stewart, P.L. Buono, and J.J. Collins. Symmetry in locomotor central pattern generators and animal gaits, *Nature* **401** (1999) 693–695.

[23] M. Golubitsky, I. Stewart, and A. Török. Patterns of synchrony in coupled cell networks with multiple arrows. *SIAM J. Appl. Dynam. Sys.* **4**(1) (2005) 78-100.

[24] J. Guckenheimer and P. Holmes. *Nonlinear Oscillations, Dynamical Systems, and Bifurcations of Vector Fields*, 3rd ed. New York: Springer-Verlag, pp. 150–154, (1997).

[25] J. Gray. *Animal Locomotion*. Weidenfeld and Nicholson, London (1968)

[26] S. Grillner. Locomotion in vertebrates: central mechanisms and reflex interaction. *Physiological Reviews* **55** (1975) 247–304.

[27] S. Grillner, J.T. Buchanan, P. Walker, and L. Brodin. Neural control of locomotion in lower vertebrates. In: *Neural Control of Rhythmic Movements in Vertebrates*, John Wiley & Sons (1988) 1–40.

[28] S. Grillner, P. Wallén, K. Saitoh, A. Kozlov, B. Robertson. Neural bases of goal-directed locomotion in vertebrates - an overview. *Brain Research Reviews* **57** (2008) 2–12.

[29] G.W. Hiebert, P.J. Whelan, A. Prochazka, and K.G. Pearson. Contribution of hind limb flexor muscle afferents to the timing of phase transitions in the cat step cycle., *J. Neurophysiology* **75** Issue 3 (1996) 1126–1137.

[30] M. Hildebrand. Symmetrical gaits of horses, *Science* **150** (1965) 701-708.

[31] Y.J. Lee, J. Lee, K.K. Kima, Y.-B. Kima, J. Ayers. Low power CMOS electronic central pattern generator design for a biomimetic underwater robot. *Neurocomputing* **71** 1-3 (2007) 284–296.

[32] M.A. Lewis, R. Etienne-Cummings, M.J. Hartmann, Z.R. Xu, and A.H. Cohen. An in silico central pattern generator: silicon oscillator, coupling, entrainment, and physical computation, *Biol. Cybern.* **88** (2003) 137–151.

[33] G.L. Liu, M.K. Habib, K. Watanabe, and K. Izumi. Central pattern generators based on Matsuoka oscillators for the locomotion of biped robots, *Artif Life Rootics* **12** (2008) 264–269.

[34] E. Marder and D. Bucher. Central pattern generators and the control of rhythmic movements, *Current Biology* **11** Issue 23 (2001) 986–996.

[35] J. Marsden, and M. McCracken. *Hopf Bifurcation and Its Applications.* New York: Springer-Verlag, (1976).

[36] V. Matos, C.P. Santos, C.M.A. Pinto. (2009) A Brainstem-like Modulation Approach for Gait Transition in a Quadruped Robot. *Proceedings of The 2009 IEEE/RSJ International Conference on Intelligent RObots and Systems, IROS 2009* St Louis, MO, USA, October (2009).

[37] O. Michel. Webots: Professional Mobile Robot Simulation. *Journal of Advanced Robotics Systems* **1** No 1 (2004) 39–42.

© 2012 European Society of Computational Methods in Sciences, Engineering and Technology (ESCMSET)

[38] M.P. Murray. Gait as a total pattern of movement. *Am J Phys Med* **46** (1967) 290-333.

[39] F. Nagashima. A motion learning method using CPG/NP. In CD *Proceedings of the 2nd International Symposium on Adaptive Motion of Animals and Machines* (2003).

[40] Y. Nakamura, T. Moria, M. Satoc, S. Ishi. Reinforcement learning for a biped robot based on a CPG-actor-critic method. *Neural Networks* **20** 6 (2007) 723–735.

[41] J. Or. A hybrid CPG-ZMP control system for stable walking of a simulated flexible spine humanoid robot. *Neural Networks* **23** Issue 3 (2010) 452–460.

[42] K.G. Pearson. Common Principles of Motor Control in Vertebrates and Invertebrates, *Annual Review of Neuroscience* **16** (1993) 265–297.

[43] C.M.A. Pinto and M. Golubitsky. Central pattern generators for bipedal locomotion. *Journal of Mathematical Biology* **53** (2006) 474–489.

[44] L. Righetti and A.J. Ijspeert. Pattern generators with sensory feedback for the control of quadruped locomotion. *IEEE International Conference on Robotics and Automation, 2008. ICRA 2008*. No 19-23 (2008) 819–824.

[45] L. Righetti and A.J. Ijspeert. Design methodologies for central pattern generators: an application to crawling humanoids. *Proceedinhs of Robotic Science and Systems* (2006) 191–198.

[46] J. Shan, F. Nagashima. Neural locomotion controller design and implementation for humanoid robot HOAP-1. *20th Annual Conference of the Robotics Society of Japan*. Robotics Society of Japan, Osaka (2002).

[47] G. Schöner, M. Dose. A dynamical systems approach to tasklevel system integration used to plan and control autonomous vehicle motion. *Robotics and Autonomous Systems* **10** (4) (1992) 253–267.

[48] A.I. Selverston. Are central pattern generators understandable? *Behav. Brain Sci.* **3** (1980) 535–571.

[49] J. Sousa, V. Matos, and C. Santos. A Bio-Inspired Postural Control for a Quadruped Robot: An Attractor-Based Dynamics. In *Procceedings of the 2010 IEEE/RSJ International Conference on Intelligent Robots and Systems*, Taipei, Taiwan (2010).

[50] I. Stewart, M. Golubitsky and M. Pivato. Symmetry groupoids and patterns of synchrony in coupled cell networks. *SIAM J. Appl. Dynam. Sys.* **2** (4) 609–646. (2003)

[51] G. Taga. Emergence of bipedal locomotion through entrainment among the neuro-musculo-skeletal system and the environment. *Physica D*, **75** (1–3) (1994) 190–208.

[52] G. Taga, Y. Yamaguchi, and H Shimizu. Self-organized control of bipedal locomotion by neural oscillators in unpredictable environment, *Biol. Cybern.* **65** (1991) 147–169.

[53] X. Wu, S. Ma. CPG-based control of serpentine locomotion of a snake-like robot. *Mechatronics*. Article in Press, Corrected Proof (2010).

[54] S.X. Yang, M. Meng. An efficient neural network approach to dynamic robot motion planning. *Neural Networks* **13** 2 (2000) 143–148.

[55] D. Zhanga, D. Hu, L. Shena, and H. Xie. Design of an artificial bionic neural network to control fish-robot's locomotion. *Neurocomputing* **71** Issues 4–6 (2008) 648–654.

© *2012 European Society of Computational Methods in Sciences, Engineering and Technology (ESCMSET)*